

Efimov Physics in ${}^6\text{Li}$ Atoms

Eric Braaten,^{1,2} H.-W. Hammer,² Daekyoung Kang,¹ and Lucas Platter¹

¹*Department of Physics, The Ohio State University, Columbus, OH 43210, USA*

²*Helmholtz-Institut für Strahlen- und Kernphysik
(Theorie) and Bethe Center for Theoretical Physics,
Universität Bonn, 53115 Bonn, Germany*

(Dated: August 2009)

Abstract

A new narrow 3-atom loss resonance associated with an Efimov trimer crossing the 3-atom threshold has recently been discovered in a many-body system of ultracold ${}^6\text{Li}$ atoms in the three lowest hyperfine spin states at a magnetic field near 895 G. O'Hara and coworkers have used measurements of the 3-body recombination rate in this region to determine the complex 3-body parameter associated with Efimov physics. Using this parameter as the input, we calculate the universal predictions for the spectrum of Efimov states and for the 3-body recombination rate in the universal region above 600 G where all three scattering lengths are large. We predict an atom-dimer loss resonance at 672 ± 2 G associated with an Efimov trimer disappearing through an atom-dimer threshold. We also predict an interference minimum in the 3-body recombination rate at 759 ± 1 G where the 3-spin mixture may be sufficiently stable to allow experimental study of the many-body system.

PACS numbers: 31.15.-p, 34.50.-s, 67.85.Lm, 03.75.Ss

Keywords: Degenerate Fermi gases, three-body recombination, scattering of atoms and molecules.

I. INTRODUCTION

Ultracold atomic gases allow the experimental study of many-body physics in systems in which the fundamental interactions are theoretically understood and experimentally controllable. There are many possibilities for the atomic constituents of the many-body system: they can be identical atoms that are all in the same spin state or there can be multiple species of constituents that are either different spin states of the same atom, different isotopes of an atom, or atoms of different elements. If the atoms are identical fermions in the same spin state, the many-body system is essentially an ideal gas. If the atoms are fermions with two spin states, there is a well-behaved zero-range limit in which the interactions are completely determined by the scattering length a . The ground state of the many-body system with equal populations of the two spin states is a superfluid. As a is changed from a negative value to a positive value through $\pm\infty$, the mechanism for superfluidity changes smoothly from the *BCS mechanism* (Cooper pairing of atoms) to the *BEC mechanism* (Bose-Einstein condensation of diatomic molecules). In the *unitary limit* in which the pair scattering length is infinitely large, the behavior of the system is constrained by *scale invariance*: invariance under rescaling space and time by arbitrary positive numbers λ and λ^2 , respectively. There have been extensive investigations, both experimental and theoretical, of the universal behavior of the system in the crossover region [1].

Fermionic atoms with three spin states open up new possibilities for universal behavior. In the many-body system, there can be new superfluid phases and new mechanisms for superfluidity [2–6]. The universal behavior can be more complex, because there are three independent scattering lengths. However it is also qualitatively different because of the *Efimov effect*. This remarkable phenomenon was discovered by Vitaly Efimov in the 3-body problem for identical bosons [7]. In the *unitary limit* in which the three pair scattering lengths are all infinitely large, there is an infinite sequence of 3-body bound states called *Efimov trimers* with an accumulation point at the 3-atom threshold. The ratio of the binding energies of successive Efimov trimers is approximately $1/515$. This geometric spectrum reflects *discrete scale invariance*: invariance under rescaling space and time by the same integer power of $\lambda_0 \approx 22.7$ and $\lambda_0^2 \approx 515$, respectively. Low-energy phenomena associated with discrete scale invariance are generally referred to as *Efimov physics* [8–10]. (See Ref. [10] for a summary of recent developments.) Efimov physics can also occur in other 3-body systems if at least two of the three pair scattering lengths are large. The discrete scaling factor depends on the mass ratios of the particles and their symmetries. In the case of fermions with 3 spin states for which the 3 pair scattering lengths are all large, the Efimov effect occurs with the same discrete scaling factor λ_0 as for identical bosons [11].

The first experimental evidence for Efimov physics in ultracold atoms was presented by Kraemer et al. [12]. Their atoms were ^{133}Cs atoms in the lowest hyperfine spin state, which are identical bosons. They observed resonant enhancement of the loss of atoms from 3-body recombination that can be attributed to an Efimov trimer crossing the 3-atom threshold. The dependence of the three-body recombination rate on the scattering length was first calculated in Refs. [13–15]. In particular, Esry, Greene and Burke predicted a resonant enhancement of the three-body recombination rate at negative values of the scattering length [14]. The universal line shape for the resonance as a function of the scattering length was first derived by Braaten and Hammer [16]. Kraemer et al. also observed a minimum in the 3-body recombination rate that can be interpreted as an interference effect associated with Efimov physics. In a subsequent experiment with a mixture of ^{133}Cs atoms and dimers, Knoop et al.

observed a resonant enhancement in the loss of atoms and dimers [17]. This loss feature can be explained by an Efimov trimer crossing the atom-dimer threshold [18]. The most exciting recent developments in the Efimov physics of ^{133}Cs atoms involve universal tetramer states. Platter and Hammer discovered that there is a pair of universal tetramer states associated with every Efimov trimer and they calculated their binding energies for limited ranges of the scattering length [19]. Von Stecher, D’Incao and Greene mapped out their spectrum for all scattering lengths and pointed out that resonant enhancement of 4-body recombination would provide a signature for these tetramers [20]. Ferlaino et al. recently observed the loss resonances from both tetramers in an ultracold gas of ^{133}Cs atoms [21].

Recent experiments with other bosonic atoms have also provided evidence of Efimov physics. Zaccanti et al. measured the 3-body recombination rate and the atom-dimer loss rate in a ultracold gas of ^{39}K atoms [22]. They observed two atom-dimer loss resonances and two minima in the 3-body recombination rate at large positive values of the scattering length. The positions of the loss features are consistent with the universal predictions with discrete scaling factor 22.7. They also observed loss features at large negative scattering lengths. Barontini et al. obtained the first evidence of the Efimov effect in a heteronuclear mixture of ^{41}K and ^{87}Rb atoms [23]. They observed 3-atom loss resonances at large negative scattering lengths in both the K-Rb-Rb and K-K-Rb channels, for which the discrete scaling factors are 131 and 3.51×10^5 , respectively. Gross et al. measured the 3-body recombination rate in an ultracold system of ^7Li atoms [24]. They observed a 3-atom loss resonance at a large negative scattering length and a 3-body recombination minimum at a large positive scattering length. The positions of the loss features, which are in the same universal region on different sides of a Feshbach resonance, are consistent with the universal predictions with discrete scaling factor 22.7.

A promising fermionic atom in which to observe Efimov physics is ^6Li . For the three lowest hyperfine states of ^6Li atoms, the three pair scattering lengths approach a common large negative value at large magnetic fields and all three have nearby Feshbach resonances at lower fields that can be used to vary the scattering lengths [25]. The first experimental studies of many-body systems of ^6Li atoms in the three lowest hyperfine states have recently been carried out by Ottenstein et al. [26] and by Huckans et al. [27]. Their measurements of the 3-body recombination rate revealed a narrow loss feature and a broad loss feature in a region of low magnetic field. Theoretical calculations of the 3-body recombination rate supported the interpretation that the narrow loss feature arises from an Efimov trimer crossing the 3-atom threshold [28–30]. Very recently, another narrow loss feature was discovered in a much higher region of the magnetic field by Williams et al. [31] and by Jochim and coworkers [32]. Williams et al. used measurements of the 3-body recombination rate in this region to determine the complex 3-body parameter that governs Efimov physics in this system. This parameter, together with the three scattering lengths as functions of the magnetic field, determine the universal predictions for ^6Li atoms in this region of the magnetic field.

In this paper, we calculate universal predictions for various aspects of Efimov physics for the three lowest hyperfine spin states of ^6Li atoms. In Section II, we explain how universal predictions for 3-body observables can be calculated efficiently by solving coupled sets of integral equations. We apply these methods specifically to the 3-body recombination rate and to the binding energies and widths of Efimov trimers. In Section III, we summarize previous experimental and theoretical work on ^6Li atoms in the universal region at low magnetic fields where all 3 scattering lengths are negative and relatively large. In Section IV, we use the complex 3-body parameter determined by Williams et al. to calculate universal predictions

for the binding energies and widths of Efimov trimers and for the three-body recombination rate in regions where one or more of the scattering lengths are large and positive. We predict an atom-dimer resonance at 672 ± 2 G where an Efimov trimer disappears through an atom-dimer threshold. We predict an interference minimum in the 3-body recombination rate at 759 ± 1 G where the 3-spin mixture may be sufficiently stable to allow experimental study of the many-body system. We also discuss the implications of our predictions for the many-body physics of ^6Li atoms. We summarize our results in Section V.

II. THEORETICAL FORMALISM

A. Fermions with Three Spin States

We consider a fermionic atom of mass m with three spin states that we label as types 1, 2, and 3. We denote the scattering length of the pair ij by either $a_{ij} = a_{ji}$ or a_k , where (ijk) is a permutation of (123) . We assume that the three pair scattering lengths $a_{12} = a_3$, $a_{23} = a_1$, and $a_{13} = a_2$ are all much larger than the range of interactions. The two-body physics for fermions with two distinct spin states that have a large pair scattering length a_{ij} is very simple in the zero-range limit. The scattering amplitude for the pair ij with relative wavenumber q is $(-1/a_{ij} - iq)^{-1}$. If a_{ij} is positive, there is a weakly-bound diatomic molecule with constituents i and j and with binding energy $\hbar^2/(ma_{ij}^2)$. We will refer to it as the (ij) *dimer*. We refer to the (12) , (23) , and (13) dimers collectively as *shallow dimers*. For realistic interactions with finite range R , there can also be deeply-bound diatomic molecules whose binding energies are comparable to or larger than the energy scale $\hbar^2/(mR^2)$ set by the range. We refer to them as *deep dimers*. Their binding energies are insensitive to changes in the large scattering lengths.

For the 3-atom problem, we take the zero of energy to be the scattering threshold for the three atoms. If a_{jk} is positive, the scattering threshold for an atom of type i and a (jk) dimer is $-\hbar^2/(ma_{jk}^2)$. We will refer to this scattering threshold as the $i + (jk)$ *atom-dimer threshold*. We will refer to triatomic molecules as *trimers*. A trimer whose constituents are atoms of types 1, 2, and 3 must have energy below the 3-atom threshold and below the $i + (jk)$ atom-dimer threshold if $a_{jk} > 0$.

The three-body physics for fermions with three distinct spin states is more complicated than for two distinct spin states, because now there are three scattering lengths a_{12} , a_{23} , and a_{13} . Depending on the signs of these scattering lengths, there can be 0, 1, 2, or 3 types of shallow dimers. The three-body physics is also much more intricate due to the Efimov effect. The unitary limit in which all three scattering lengths are infinitely large is characterized by discrete scale invariance with discrete scaling factor $\lambda_0 = e^{\pi/s_0} \approx 22.7$, where $s_0 \approx 1.00624$ is a transcendental number. This requires a 3-body parameter that provides another length scale in addition to the three scattering lengths. If there were no such parameter, the system would have continuous scale invariance in the unitary limit.

One simple choice for the 3-body parameter is a wavenumber κ_* defined by the spectrum of 3-body bound states (*Efimov trimers*) in the unitary limit in which all three scattering lengths are infinite [8]. Their binding energies relative to the 3-atom threshold are

$$E_T^{(n)} = \lambda_0^{2(n_*-n)} \frac{\hbar^2 \kappa_*^2}{m} \quad (a_{12} = a_{23} = a_{31} = \pm\infty), \quad (1)$$

where κ_* is the binding wavenumber of the trimer labeled n_* and n is an integer. There

are infinitely many of these Efimov trimers with an accumulation point at the threshold for three atoms of types 1, 2, and 3. The advantage of using the Efimov parameter κ_* as the 3-body parameter is that physical observables must be log-periodic functions of κ_* . In the zero-range limit, the Efimov spectrum also extends infinitely deep to $-\infty$. For finite range R , the deepest Efimov trimer may have a binding energy E_T as large as $\hbar^2/(mR^2)$. However, universal predictions will be accurate only if its binding energy is significantly smaller, because range corrections are expected to be of order $R(mE_T/\hbar^2)^{1/2}$.

In the unitary limit, the Efimov states are sharp states with the spectrum in Eq. (1) only if there are no deep dimers in any of the three 2-body channels. If there are deep dimers, their inclusive effects can be taken into account by analytically continuing the Efimov parameter κ_* to a complex value that is conveniently expressed in the form $\kappa_* \exp(i\eta_*/s_0)$, where κ_* and η_* are positive real parameters [16]. Making the substitution $\kappa_* \rightarrow \kappa_* \exp(i\eta_*/s_0)$ on the right side of Eq. (1), we find that the Efimov trimers acquire nonzero decay widths $\Gamma_T^{(n)}$. The binding energies and widths are

$$E_T^{(n)} = \lambda_0^{2(n_*-n)} \frac{\hbar^2 \kappa_*^2 \cos(2\eta_*/s_0)}{m} \quad (a_{12} = a_{23} = a_{31} = \pm\infty), \quad (2)$$

$$\Gamma_T^{(n)} = \lambda_0^{2(n_*-n)} \frac{2\hbar^2 \kappa_*^2 \sin(2\eta_*/s_0)}{m}. \quad (3)$$

B. Three-body Recombination

Three-body recombination is a three-atom collision in which two of the atoms form a dimer. In the case of three fermions in the same spin state, 3-body recombination is strongly suppressed at low temperature, because each pair of atoms has only P-wave interactions. In the case of two fermions of type i and a third atom of a different type j , two of the pairs have S-wave interactions with scattering length a_{ij} . The rate for 3-body recombination in the zero-range limit still decreases to 0 as the energy E of the atoms approaches the threshold, decreasing like E if $a_{ij} > 0$ [33] and like E^3 if $a_{ij} < 0$ [34]. In the case of three distinct spin states, all three pairs of atoms can have S-wave interactions. There is no threshold suppression of three-body recombination if at least two of the three scattering lengths are large. If a_{ij} is large and positive, one of the recombination channels is into the (ij) dimer and a recoiling atom with complimentary spin k . If there are deep dimers in any of the three 2-body channels, they provide additional recombination channels. If all three scattering lengths are negative, the only recombination channels are into deep dimers.

The rate equations for the number densities n_i of atoms in the three spin states are

$$\frac{d}{dt}n_i = -K_3 n_1 n_2 n_3. \quad (4)$$

The event rate constant K_3 can be separated into the inclusive rate constant K_3^{deep} for recombination into deep dimers and the exclusive rate constants $K_3^{(ij)}$ for recombination into each of the three possible shallow dimers:

$$K_3 = K_3^{\text{deep}} + K_3^{\text{shallow}}, \quad (5)$$

$$K_3^{\text{shallow}} = K_3^{(12)} + K_3^{(23)} + K_3^{(13)}. \quad (6)$$

The term $K_3^{(ij)}$ is nonzero only if $a_{ij} > 0$.

In the low-temperature limit, the rate constant K_3 and the exclusive rate constants $K_3^{(ij)}$ can be expressed in terms of T-matrix elements for processes in which the initial state consists of three atoms in the spin states 1, 2, and 3 with momentum $\mathbf{0}$. By the optical theorem, K_3 is twice the imaginary part of the forward T-matrix element for 3-atom elastic scattering in the limit where the momenta of the atoms all go to 0:

$$K_3 = 2 \operatorname{Im} \mathcal{T}(\mathbf{0}, \mathbf{0}, \mathbf{0}; \mathbf{0}, \mathbf{0}, \mathbf{0}). \quad (7)$$

The T-matrix element is singular as all the momenta go to zero, but its imaginary part is not. If $a_{ij} > 0$, the rate constant $K_3^{(ij)}$ for recombination into the (ij) dimer is the square of the T-matrix element for three atoms with momentum $\mathbf{0}$ to scatter into the dimer and a recoiling atom multiplied by the atom-dimer phase space:

$$K_3^{(ij)} = \frac{4m}{3\sqrt{3}\pi\hbar a_k} |\mathcal{T}_k(\mathbf{0}, \mathbf{0}, \mathbf{0}; \mathbf{p}, -\mathbf{p})|^2 \Big|_{|\mathbf{p}|=2\hbar/(\sqrt{3}a_k)}. \quad (8)$$

The dimer and the recoiling atom with complementary spin k both have momentum $2\hbar/(\sqrt{3}a_k)$. For convenience, we will switch to wavenumber variables in the remainder of the paper.

The T-matrix elements in Eqs. (7) and (8) can be expressed in terms of amplitudes $\mathcal{A}_{ij}(p, q; E)$ for the transition from an atom of type i and a complimentary diatom pair into an atom of type j and a complimentary diatom pair, with the two diatom pairs being the first to interact and the last to interact, respectively. The projection onto S-waves reduces the amplitude to a function of three variables: the relative wavenumber p of the incoming atom and diatom, the relative wavenumber q of the outgoing atom and diatom, and the total energy E of either the incoming atom and diatom or the outgoing atom and diatom. The rate constant K_3 in Eq. (7) can be expressed as

$$K_3 = \frac{32\pi^2\hbar}{m} \sum_{i,j} a_i a_j \operatorname{Im} \mathcal{A}_{ij}(0, 0; 0), \quad (9)$$

where the sums are over $i, j = 1, 2, 3$. The exclusive rate constant in Eq. (8) for 3-body recombination into the (ij) dimer can be expressed as

$$K_3^{(ij)} = \frac{512\pi^2\hbar}{3\sqrt{3}ma_k^2} \left| \sum_l a_l \mathcal{A}_{lk}(0, 2/(\sqrt{3}a_k); 0) \right|^2, \quad (10)$$

where k is the complimentary spin to ij and the sum is over $l = 1, 2, 3$.

C. STM Equations

The 9 amplitudes $\mathcal{A}_{ij}(p, q; E)$ satisfy coupled integral equations in the variable q that are generalizations of the Skorniakov–Ter-Martirosian (STM) equation [35]. To determine the rate constants for 3-body recombination in Eqs. (9) and (10), it is sufficient to set the relative wavenumber in the initial state to 0 and the total energy to 0. The 9 coupled STM equations for $\mathcal{A}_{ij}(0, p; 0)$ are [28]

$$\mathcal{A}_{ij}(0, p; 0) = \frac{1 - \delta_{ij}}{p^2} + \frac{2}{\pi} \sum_k (1 - \delta_{kj}) \int_0^\Lambda dq Q(p, q; 0) D_k(3q^2/4) \mathcal{A}_{ik}(0, q; 0), \quad (11)$$

where

$$Q(p, q; E) = \frac{q}{2p} \log \frac{p^2 + pq + q^2 - mE/\hbar^2}{p^2 - pq + q^2 - mE/\hbar^2}, \quad (12)$$

$$D_k(p^2) = \left[-1/a_k + \sqrt{p^2 - i\epsilon} \right]^{-1}, \quad (13)$$

and Λ is an ultraviolet cutoff that must be large compared to p , $1/|a_1|$, $1/|a_2|$, and $1/|a_3|$. Since the T-matrix elements in Eqs. (9) and (10) involve only the three linear combinations $\sum_i a_i \mathcal{A}_{ij}(0, p; 0)$, the 9 coupled STM equations can be reduced to 3 coupled integral equations for these 3 linear combinations. If Λ is sufficiently large, the solutions to the integral equations in Eqs. (11) depend only log-periodically on Λ with a discrete scaling factor $\lambda_0 \approx 22.7$. The dependence on the arbitrary cutoff Λ can be eliminated in favor of a physical 3-body parameter, such as the Efimov parameter κ_* defined by Eq. (1). If we restrict Λ to a range that corresponds to a multiplicative factor of 22.7, then Λ differs from κ_* only by a multiplicative numerical constant. Thus, we can also simply use Λ as the 3-body parameter [36].

If Λ is real valued, the STM equations describe atoms that have no deep dimers. The rate K_3^{deep} for 3-body recombination into deep dimers, which can be obtained by combining Eqs. (5), (6), (9), and (10), must therefore be zero. For atoms that have deep dimers, the effects of the deep dimers can be described indirectly by using a complex-valued 3-body parameter. If we use the ultraviolet cutoff Λ as the 3-body parameter, the inclusive effects of deep dimers can be taken into account by analytically continuing the upper endpoint of the integral Λ in Eqs. (11) to a complex value $\Lambda \exp(i\eta_*/s_0)$. The path of integration in the variable q can be taken to run along the real axis from 0 to Λ and then along the arc from Λ to $\Lambda \exp(i\eta_*/s_0)$. This path can be deformed to run along the straight line from 0 to $\Lambda \exp(i\eta_*/s_0)$ provided we add explicitly the contributions from any poles that are crossed as the contour is deformed. These poles arise from the diatom propagator $D_k(p^2)$, which in the case $a_k > 0$ has a pole associated with the shallow dimer at $p = 1/a_k$. For example, if $a_k > 0$, the integral in Eq. (11) with a complex ultraviolet cutoff $\Lambda e^{i\eta_*/s_0}$ can be written

$$\begin{aligned} & \left(\int_0^\Lambda dq + \int_\Lambda^{\Lambda e^{i\eta_*/s_0}} dq \right) Q(p, q; 0) D_k(3q^2/4) \mathcal{A}_{ik}(0, q; 0) \\ &= Q(p, q_k; 0) \frac{4\pi i}{\sqrt{3}} \mathcal{A}_{ik}(0, q_k; 0) + \int_0^{\Lambda e^{i\eta_*/s_0}} dq Q(p, q; 0) D_k(3q^2/4) \mathcal{A}_{ik}(0, q; 0), \end{aligned} \quad (14)$$

where $q_k = 2/(\sqrt{3}a_k)$. In the integral on the right side, the integration contour runs along the straight line path from 0 to $\Lambda e^{i\eta_*/s_0}$. With the ultraviolet cutoff replaced by $\Lambda \exp(i\eta_*/s_0)$, the rate K_3^{deep} for 3-body recombination into deep dimers is nonzero.

The rate constant K_3 in Eq. (9) requires the extrapolation of the solutions $\mathcal{A}_{ij}(0, p; 0)$ to the STM equations in Eqs. (11) to $p = 0$. These solutions are singular as $p \rightarrow 0$. The singular terms, which are proportional to $1/p^2$, $1/p$, and $\ln p$, appear only in $\text{Re } \mathcal{A}_{ij}(0, p; 0)$ for real p and can be derived by iterating the integral equations [37]. Since $\text{Im } \mathcal{A}_{ij}(0, p; 0)$ must be extrapolated to $p = 0$, it is useful to transform Eqs. (11) into coupled STM equations for

amplitudes $\bar{\mathcal{A}}_{ij}(0, p; 0)$ obtained by subtracting the singular terms from $\mathcal{A}_{ij}(0, p; 0)$:

$$\begin{aligned} \bar{\mathcal{A}}_{ij}(0, p; 0) = \mathcal{A}_{ij}(0, p; 0) &- \frac{1 - \delta_{ij}}{p^2} + \frac{\pi}{3p} \sum_n a_n (1 - \delta_{in})(1 - \delta_{nj}) \\ &- \log \frac{p}{\Lambda} \left\{ \frac{\sqrt{3}}{\pi} \sum_n a_n^2 (1 - \delta_{in})(1 - \delta_{nj}) \right. \\ &\quad \left. - \frac{2}{3} \sum_{m,n} a_m a_n (1 - \delta_{im})(1 - \delta_{mn})(1 - \delta_{nj}) \right\}. \end{aligned} \quad (15)$$

D. Three Equal Scattering Lengths

We can obtain analytic results for the 3-body recombination rate in the case of three equal scattering lengths: $a_{12} = a_{23} = a_{13} = a$. In this case, the 3-body recombination rates in Eqs. (9) and (10) depend only on the combination $\sum_i \mathcal{A}_{ij}(0, p; 0)$. One can show that the solutions to the STM equation for $\sum_i \mathcal{A}_{ij}(p, q; E)$ are the same for $j = 1, 2, 3$ and are equal to the corresponding amplitude $\mathcal{A}(p, q; E)$ for identical bosons with scattering length a :

$$\sum_i \mathcal{A}_{ij}(p, q; E) = \mathcal{A}(p, q; E), \quad j = 1, 2, 3. \quad (16)$$

The STM equation analogous to Eq. (11) for identical bosons is¹

$$\mathcal{A}(0, p; 0) = \frac{2}{p^2} + \frac{4}{\pi} \int_0^\Lambda dq Q(p, q; 0) D(3q^2/4) \mathcal{A}(0, q; 0). \quad (17)$$

If the low-temperature limit is taken with the number density for the identical bosons much smaller than the critical density for Bose-Einstein condensation, the rate constant for 3-body recombination of identical bosons into the shallow dimer is [8]

$$K_3^{\text{shallow}} = \frac{512\pi^2 \hbar}{\sqrt{3}m} \left| \mathcal{A}(0, 2/(\sqrt{3}a); 0) \right|^2. \quad (18)$$

Upon making the substitution $\sum_l a_l \mathcal{A}_{lk} \rightarrow a \mathcal{A}$ in Eq. (10), we see that the recombination rate $K_3^{(ij)}$ for the three fermions into the (ij) dimer is exactly 1/3 of the recombination rate for identical bosons in Eq. (18). Summing over the three shallow dimers, we find that the expression for the recombination rate of the three fermions into shallow dimers is identical to the expression for the recombination rate of identical bosons into the single shallow dimer. Similarly, we find that the expression in Eq. (9) for the total recombination rate of the three fermions is identical to that for the total recombination rate of identical bosons.

Braaten and Hammer deduced a semi-analytic expression for the rate constant for 3-body recombination of identical bosons into deep dimers with a large negative scattering length a [16]:

$$K_3^{\text{deep}} = \frac{16\pi^2 C \sinh(2\eta_*)}{\sin^2[s_0 \ln(a/a'_*)] + \sinh^2 \eta_*} \frac{\hbar a^4}{m} \quad (a < 0), \quad (19)$$

¹ The amplitude $\mathcal{A}(p, q; E)$ differs from the amplitude $\mathcal{A}_S(p, q; E)$ in Ref. [8] by a multiplicative factor of $a/(8\pi)$.

where $s_0 = 1.00624$, $a'_* = -1/(D\kappa_*)$, and C and D are numerical constants. The most accurate values for the numerical constants are $C = 29.62(1)$ and $D = 0.6642(2)$ [28, 38]. The relation between the Efimov parameter and the ultraviolet cutoff is $\kappa_* = 0.17609(5)\Lambda$, modulo multiplication by an integer power of $\lambda_0 \approx 22.7$. The expression for the recombination rate constant in Eq. (19) exhibits resonant enhancement for a near the values $\lambda_0^n a_*$ for which there is an Efimov trimer at the 3-body threshold. The line shape in Eq. (19) for the 3-atom loss resonance as a function of the scattering length played a key role in the discovery of an Efimov state for ^{133}Cs atoms in the lowest hyperfine state [12]. It applies equally well to three fermions with equal negative pair scattering lengths.

Macek, Ovchinnikov, and Gasaneo [39] and Petrov [40] have deduced a completely analytic expression for the 3-body recombination rate constant for identical bosons with a large positive scattering length a in the case where there are no deep dimers. Braaten and Hammer generalized their result to the case where there are deep dimers by making the analytic continuation $\kappa_* \rightarrow \kappa_* \exp(i\eta_*/s_0)$ in the amplitude for this process [9]. The resulting analytic expression for the recombination rate is [9]

$$K_3^{\text{shallow}} = \frac{128\pi^2(4\pi - 3\sqrt{3})(\sin^2[s_0 \ln(a/a_{*0})] + \sinh^2 \eta_*)}{\sinh^2(\pi s_0 + \eta_*) + \cos^2[s_0 \ln(a/a_{*0})]} \frac{\hbar a^4}{m} \quad (a > 0), \quad (20)$$

where $a_{*0} \approx 0.32 \kappa_*^{-1}$. This expression exhibits minima for a near the values $\lambda_0^n a_{*0}$ arising from destructive interference between two pathways for recombination. This formula applies equally well to three fermions with equal positive pair scattering lengths. It gives the recombination rate K_3^{shallow} in Eq. (6), which is summed over the 3 shallow dimers.

E. Efimov Trimers

The transition amplitudes $\mathcal{A}_{ij}(p, q; E)$ have poles in the total energy E at the energies $E^{(n)}$ of the Efimov trimers. Near the pole, the amplitudes factor:

$$\mathcal{A}_{ij}(p, q; E) \longrightarrow \frac{\mathcal{B}_i(p)^* \mathcal{B}_j(q)}{E - E^{(n)}}. \quad (21)$$

The spectrum of Efimov trimers can be obtained by solving the three coupled homogeneous integral equations for $\mathcal{B}_j(q)$:

$$\mathcal{B}_j(p) = \frac{2}{\pi} \sum_k (1 - \delta_{kj}) \int_0^\Lambda dq Q(p, q; E) D_k(3q^2/4 - mE/\hbar^2) \mathcal{B}_k(q), \quad (22)$$

where the ultraviolet cutoff Λ must be much larger than p , $|mE/\hbar^2|^{1/2}$, and all three inverse scattering lengths $1/a_i$. The set of homogeneous STM equations in Eq. (22) are nonlinear eigenvalue equations for E . If Λ is real valued, the eigenvalues are real valued if the energy is below all the scattering thresholds. The Efimov trimers are therefore sharp states with 0 widths. There is always a 3-atom scattering threshold at $E = 0$. If $a_{ij} > 0$, the atom-dimer scattering threshold at $E = -\hbar^2/(ma_{ij}^2)$ has lower energy.

If there are deep dimers, the Efimov trimers can decay into a deep dimer and a recoiling atom. Their widths can be calculated by analytically continuing the upper endpoint of the integral Λ in Eqs. (22) to a complex value $\Lambda \exp(i\eta_*/s_0)$. The complex energy eigenvalue for the trimer can be expressed as

$$E^{(n)} = -E_T^{(n)} - i\Gamma_T^{(n)}/2. \quad (23)$$

If $\Gamma_T^{(n)}$ is small compared to the difference between $E_T^{(n)}$ and the nearest scattering threshold, then $E_T^{(n)}$ and $\Gamma_T^{(n)}$ can be interpreted as the binding energy and the width of the trimer, respectively. If $\Gamma_T^{(n)}$ is not small, they do not have such precise interpretations.

If $\eta_* \ll 1$, the binding energies and widths of the Efimov trimers can be calculated approximately by solving the STM equation with a real-valued cutoff Λ . The complex energy $E^{(n)}$ in Eq. (23) is a function of the complex parameter $\Lambda \exp(i\eta_*/s_0)$ that must be real valued in the limit $\eta_* \rightarrow 0$. Expanding that function in powers of η_* , we find that the leading approximations to the binding energy and the width are

$$E_T^{(n)} \approx -E^{(n)} \Big|_{\eta_*=0}, \quad (24)$$

$$\Gamma_T^{(n)} \approx -\frac{2\eta_*}{s_0} \Lambda \frac{\partial}{\partial \Lambda} E^{(n)} \Big|_{\eta_*=0}. \quad (25)$$

The derivative with respect to Λ in Eq. (25) is calculated with the scattering lengths a_{ij} held fixed. The leading corrections to Eqs. (24) and (25) are suppressed by a factor of η_*^2 .

F. Dimer Relaxation

If our system of fermionic atoms is a mixture of (jk) dimers and atoms of type i , another 3-atom loss process is dimer relaxation: the inelastic scattering of the atom and the (jk) dimer into an atom and a dimer with a larger binding energy. If i coincides with j so there are only two distinct spin states, the dimer relaxation rate decreases as $a_{ik}^{-3.33}$ as the scattering length increases [41]. The atom-dimer mixture is therefore remarkably stable when the scattering length is very large. This stability was verified in the recent experiments with ^6Li atoms [26, 27]. If i is distinct from both j and k so there are three distinct spin states, there is no Pauli suppression of the atom-dimer relaxation rate. The rate increases as the scattering lengths are increased. On top of that, there can also be resonant enhancement associated with Efimov physics.

To be definite, we consider a mixture of (23) dimers and atoms of type 1. We denote the number densities of atoms and (23) dimers by n_1 and $n_{(23)}$, respectively. The loss rate from atom-dimer relaxation can be expressed in terms of a rate constant $\beta_{1(23)}$:

$$\frac{d}{dt}n_1 = \frac{d}{dt}n_{(23)} = -\beta_{1(23)}n_1n_{(23)}. \quad (26)$$

Atom-dimer relaxation channels are also inelastic atom-dimer scattering channels. So if $\beta_{1(23)} > 0$, the atom-dimer scattering length $a_{1(23)}$ must have a negative imaginary part. These two quantities are related by the optical theorem:

$$\beta_{1(23)} = -\frac{6\pi\hbar}{m} \text{Im}(a_{1(23)}). \quad (27)$$

If the scattering lengths are all large, then by dimensional analysis, $\beta_{1(23)}$ must be $\hbar a_{23}/m$ multiplied by a dimensionless coefficient that depends on the ratios of scattering lengths a_{12}/a_{23} and a_{13}/a_{23} and also on $a_{23}\kappa_*$, where κ_* is the Efimov parameter. The dependence on $a_{23}\kappa_*$ is required to be log-periodic with discrete scaling factor $\lambda_0 \approx 22.7$. The universal predictions for dimer relaxation rates can be calculated by solving appropriate sets of coupled

STM equations. The dimensionless coefficient of $\hbar a_{23}/m$ in the relaxation rate constant $\beta_{1(23)}$ can be especially large if there is an Efimov trimer close to the $1+(23)$ atom-dimer threshold. In this case, there is resonant enhancement of the dimer relaxation rate. The resulting loss feature is called an *atom-dimer loss resonance*.

III. ^6Li ATOMS: LOW-FIELD UNIVERSAL REGION

In this section, we apply our formalism to the lowest three hyperfine spin states of ^6Li atoms in the region of low magnetic field from 0 to 600 G.

A. Lowest Hyperfine Spin States of ^6Li Atoms

An example of a fermion with three spin states is ^6Li atoms in the three lowest hyperfine spin states. They can be labelled by their hyperfine quantum numbers $|f, m_f\rangle$ or by integers: $|1\rangle = |\frac{1}{2}, +\frac{1}{2}\rangle$, $|2\rangle = |\frac{1}{2}, -\frac{1}{2}\rangle$, and $|3\rangle = |\frac{3}{2}, -\frac{3}{2}\rangle$. The pair scattering lengths a_{12} , a_{23} , and a_{13} have Feshbach resonances near 834 G, 811 G, and 690 G, respectively [25]. Beyond these Feshbach resonances, all three scattering lengths approach the triplet scattering length $-2140 a_0$, which is large and negative. A convenient conversion constant for ^6Li atoms is $\hbar/m = 1.0558 \times 10^{-4} \text{ cm}^2/\text{s}$.

The relevant range for ultracold atoms is the van der Waals length $\ell_{\text{vdW}} = (mC_6/\hbar^2)^{1/4}$, which is approximately $62.5 a_0$ for ^6Li . The corresponding energy scale is the van der Waals energy $E_{\text{vdW}} = \hbar^2/(m\ell_{\text{vdW}}^2)$. The associated frequency is $\nu_{\text{vdW}} = E_{\text{vdW}}/(2\pi\hbar) \approx 154 \text{ MHz}$. The zero-range approximation should be accurate if $|a_{12}|$, $|a_{23}|$, and $|a_{13}|$ are all much larger than ℓ_{vdW} and it should be at least qualitatively useful if $|a_{ij}| > 2\ell_{\text{vdW}}$. There are two regions of the magnetic field in which all three scattering lengths are larger than $2\ell_{\text{vdW}} \approx 125 a_0$: a low-field region $122 \text{ G} < B < 485 \text{ G}$ and a high-field region $B > 608 \text{ G}$. These two universal regions are separated by a nonuniversal region in which all three scattering lengths go through zeros. Efimov physics in the universal regions will be characterized by values of κ_* and η_* that may not be the same in the two regions. In general, these parameters may be expected to vary slowly with the magnetic field, just like the scattering length away from a Feshbach resonance. In a sufficiently narrow region of magnetic field, they can be treated as constants. While their values could in principle be calculated from microscopic atomic physics, in practice they have to be determined by measurements of 3-body observables.

In Fig. 1, the three scattering lengths a_{12} , a_{23} , and a_{13} are shown as functions of the magnetic field in the low-energy region from 0 to 600 G [42]. Throughout most of this region, the smallest scattering length is a_{12} . It satisfies $|a_{12}| > 2\ell_{\text{vdW}}$ in the interval $122 \text{ G} < B < 485 \text{ G}$ and achieves its largest value $-290 a_0 = -4.6 \ell_{\text{vdW}}$ near 320 G. This interval therefore contains a universal region in which all three scattering lengths are negative and relatively large. The zero-range approximation should be quantitatively useful in the middle of this interval, but it becomes increasingly questionable as one approaches the edges.

B. Three-body Recombination

The first measurements of the 3-body recombination rate K_3 for the three lowest hyperfine spin states of ^6Li atoms were carried out by Ottenstein et al. [26] and by Huckans et al. [27].

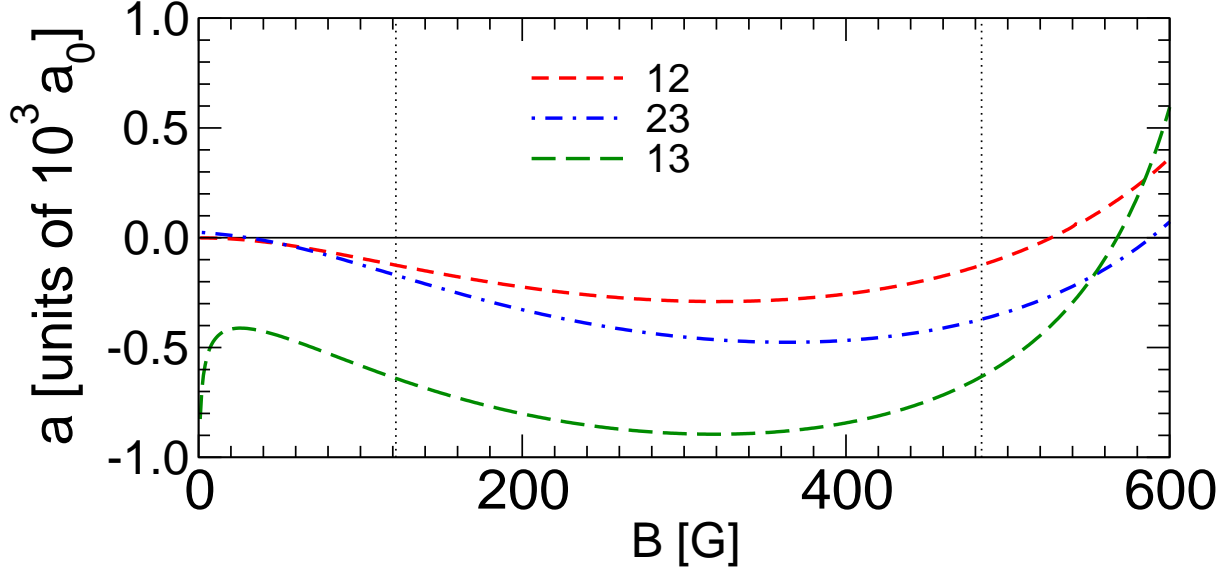


FIG. 1: (Color online) The scattering lengths in units of $10^3 a_0$ for the three lowest hyperfine states of ^6Li as functions of the magnetic field B from 0 to 600 G [42]. The two vertical dotted lines mark the boundaries of the region in which the absolute values of all three scattering lengths are greater than $2 \ell_{\text{vdW}}$.

Their results for magnetic field in the region from 0 to 600 G are shown in Fig. 2. The results for K_3 in Ref. [26] from measurements of the loss rates of the three individual spin states have been averaged to get a single value of K_3 at each value of B . Both groups observed dramatic variations in K_3 with B , including a narrow loss feature near 130 G and a broader loss feature near 500 G.

The narrow loss feature and the broad loss feature in the measurements of Refs. [26, 27] both appear near the boundaries of the region in which all three scattering lengths satisfy $|a_{ij}| > 2\ell_{\text{vdW}}$. The effects of the finite range of the interaction may be significant near the boundaries of this region. In Ref. [28], we fit the data for K_3 in this region by calculating the 3-body recombination rate K_3^{deep} in Eq. (9), using the magnetic field dependence of the three scattering lengths shown in Fig. 1 and treating Λ and η_* as fitting parameters. Since the systematic error in the normalization of K_3 was estimated to be 90% in Ref. [26] and 70% in Ref. [27], we only fit the shape of the data and not its normalization. A 3-parameter fit to the data from Ref. [26] in the region $122 \text{ G} < B < 485 \text{ G}$ with an adjustable normalization factor determines the 3-body parameters $\Lambda = 436 a_0^{-1}$ and $\eta_* = 0.11$. This value of the cutoff is equivalent to $\kappa_* = 76.8 a_0^{-1}$. These parameters κ_* and η_* determine the normalization of K_3^{deep} , so the theoretical curve in Fig. 2 is absolutely normalized. The fit to the shape of the narrow loss feature is excellent. The normalization is also correct to within the systematic error in the data. However the fit predicts that K_3 should be almost constant in the middle of the low-field region and that there should be another narrow loss feature at its upper end near 500 G. These predictions are not consistent with the data in Fig. 2, which increases monotonically in the middle of the low-field region and has a broad loss feature near the upper end of this region.

Similar results for the 3-body recombination rate of ^6Li atoms were obtained subsequently by two other groups [29, 30]. Naidon and Ueda used hyperspherical methods to calculate

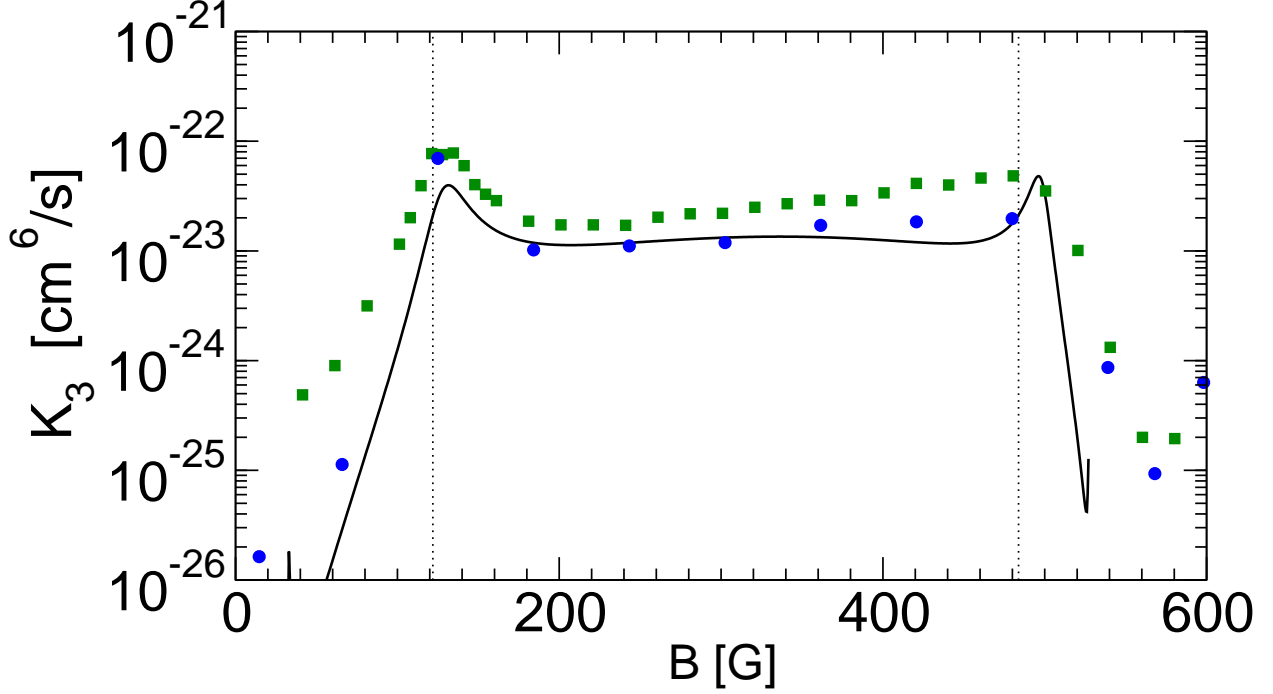


FIG. 2: (Color online) Three-body recombination rate constant K_3 as a function of the magnetic field B from 0 to 600 G. The solid squares and dots are data points from Refs. [26] and [27], respectively. The curve is the absolutely normalized result for K_3^{deep} with $\kappa_* = 76.8 a_0^{-1}$ and $\eta_* = 0.11$. The two vertical dotted lines mark the boundaries of the region in which the absolute values of all three scattering lengths are greater than $2 \ell_{\text{vdW}}$.

the recombination rate [29]. For their 3-body parameters, they used the real and imaginary parts of the logarithmic derivative of the hyperradial wavefunction. Schmidt, Floerchinger, and Wetterich used functional renormalization methods to calculate the recombination rate [30]. For their 3-body parameters, they used the real and imaginary parts of the detuning energy of a triatomic molecule. The results of both groups for K_3 as a function of the magnetic field are similar to our results in Fig. 2. One difference is that in Refs. [29, 30] the recombination rate was calculated only up to an overall normalization constant that was determined by fitting the data. In our calculation, the absolute normalization is determined by the 3-body parameters κ_* and η_* .

In Ref. [43], Wenz et al. provided an explanation for the loss feature near 500 G being much broader than predicted in Refs. [28–30]. They pointed out that there are deep dimers whose binding energies vary significantly over the low-field region. These dimers are those responsible for the Feshbach resonances 690 G, 811 G, and 834 G. In the high-field region, they are shallow dimers, but they become deep dimers in the low-field region. Their binding energies change over the low-field universal region by as much as a factor of 6. Wenz et al. assumed that contributions to the 3-body parameter η_* scale like the inverse of the binding energy of the deep dimer. They used the coefficient in this scaling relation as a fitting parameter along with the 3-body parameter equivalent to κ_* . They obtained an excellent fit to K_3 over the entire low-field region, including the narrow loss feature, the broad loss feature, and the monotonic rise in between. Their assumption for the scaling of η_* with the binding energy of the deep dimer can be justified by an explicit calculation in a two-channel

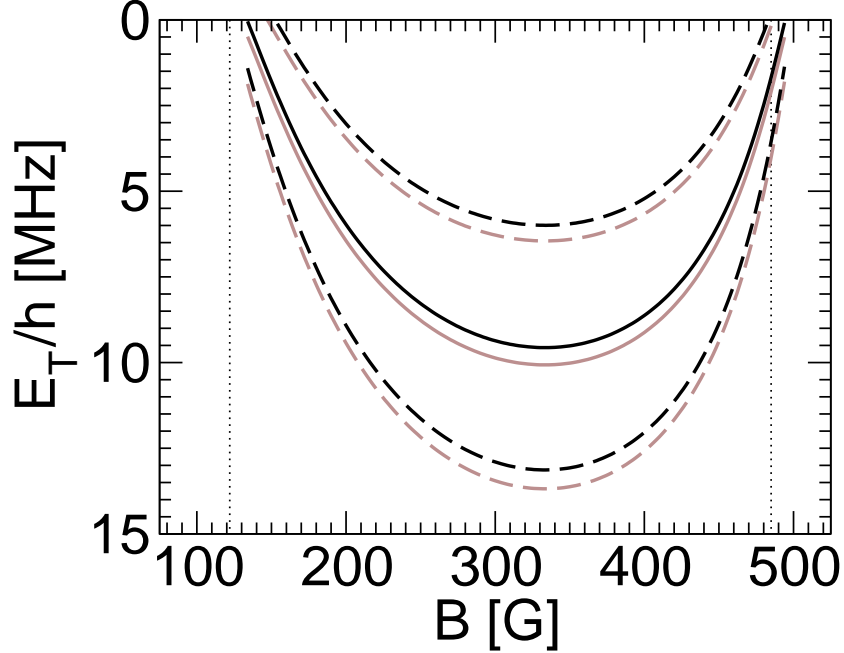


FIG. 3: (Color online) Energy of the Efimov trimer as a function of the magnetic field B in the low-field region. The binding frequency $E_T^{(1)}/(2\pi\hbar)$ (dark solid line) and the frequency $\Gamma_T^{(1)}/(2\pi\hbar)$ associated with the width (difference between dark dashed lines) were obtained from the complex energy eigenvalue calculated using the parameters $\kappa_* = 76.8 \, a_0^{-1}$ and $\eta_* = 0.11$. Also shown for comparison are the small- η_* approximation in Eqs. (24) and (25) for the binding frequency (light solid line) and for the frequency associated with the width (difference between light dashed lines). The two vertical dotted lines mark the boundaries of the region in which the absolute values of all three scattering lengths are greater than $2 \, \ell_{\text{vdW}}$.

model [44].

In Ref. [43], Wenz et al. proposed a simple analytic approximation for the 3-body recombination rate in regions where all 3 scattering lengths are negative. Their approximation is the analytic result for equal scattering lengths in Eq. (19), with a replaced by an effective scattering length a_m given by

$$a_m = - \left[(a_1^2 a_2^2 + a_2^2 a_3^2 + a_3^2 a_1^2) / 3 \right]^{1/4}. \quad (28)$$

Another possible choice for an effective scattering length is the geometric mean of the three scattering lengths:

$$a_g = -|a_1 a_2 a_3|^{1/3}. \quad (29)$$

We can use our universal results to test the accuracy of that approximation. We find that the analytic result in Eq. (19) with a replaced by the geometric mean a_g in Eq. (29) is a significantly more accurate approximation.

C. Efimov Trimers

Naidon and Ueda [29] and Schmidt, Floerchinger, and Wetterich [30] calculated the binding energy of the Efimov trimer that is responsible for the loss features in Fig. 2. Its binding

energy goes to 0 near both the observed narrow loss feature near 130 G and the predicted narrow loss feature near 500 G. This demonstrates explicitly that both loss features arise from the same Efimov trimer crossing the 3-atom threshold.

We calculate the spectrum of Efimov trimers by solving for the complex energy eigenvalues of the homogeneous STM equations in Eq. (22). The energies and widths of the trimers are obtained by expressing the complex energies in the form $-E_T^{(n)} - i\Gamma_T^{(n)}/2$. We choose to label the Efimov trimer responsible for the narrow loss feature near 135 G by the integer $n = 1$. Our predictions for the binding energy $E_T^{(1)}$ of the shallowest Efimov state are shown in Fig. 3 as a function of the magnetic field. The binding frequency $E_T^{(1)}/(2\pi\hbar)$ increases from 0 at 134 G to a maximum of 9.56 MHz at 334 G and then decreases to 0 at 494 G. Our maximum binding frequency agrees well with the maximum frequencies of about 10 MHz and about 11 MHz obtained in Refs. [29] and [30], respectively. The binding frequency $E_T^{(0)}/(2\pi\hbar)$ associated with the next deeper Efimov trimer is predicted to change gradually from 12.1 GHz at 134 G to 12.5 GHz at 334 G and then to 12.1 GHz at 494 G. Since this binding energy is much larger than the van der Waals frequency $\nu_{vdW} = 154$ MHz, this Efimov trimer and all the deeper ones predicted by the STM equations are artifacts of the zero-range approximation. Our value of κ_* can be interpreted as the binding wavenumber $(mE_T^{(-2)}/\hbar^2)^{1/2}$ of the fictitious Efimov trimer labelled by $n = -2$. It corresponds to the choice $n_* = -2$ in Eq. (1).

We note that the finite range corrections to the binding energies of the deeper trimers can be substantial if their energy becomes comparable to the van der Waals energy even if all scattering lengths are large. The leading corrections to the binding energy for the deep trimers are of order $\ell_{vdW}(mE_T^{(n)}/\hbar^2)^{1/2}$. For the trimer labeled $n = 1$, these corrections are 25% for the largest value of the binding energy.

In Ref. [29], Naidon and Ueda also calculated the width of the Efimov trimer. In Fig. 3, our results for the width $\Gamma_T^{(1)}$ are illustrated by plotting the frequencies associated with the energies $E_T^{(1)} \pm \Gamma_T^{(1)}/2$ as functions of the magnetic field. The frequency $\Gamma_T^{(1)}/(2\pi\hbar)$ increases from 2.73 MHz at 134 G to a maximum of 7.14 MHz at 332 G and then decreases to 2.56 MHz at 494 G. Our maximum width is more than twice as large as the maximum width of about $(3 \text{ MHz}) \times 2\pi\hbar$ obtained in Ref. [29]. Since our result for $\Gamma_T^{(1)}$ is always comparable to or larger than $E_T^{(1)}$, the interpretations of $E_T^{(1)}$ and $\Gamma_T^{(1)}$ as the binding energy and width of the trimer should be viewed with caution.

Since $\eta_* = 0.11$ is relatively small, we can also use the small- η_* approximations to the binding energy and the width given in Eqs. (25) and (24). These approximations, which are calculated using $\kappa_* = 76.8 \text{ } a_0^{-1}$, are shown in Fig. 3 for comparison. The maximum binding frequency $E_T^{(1)}/(2\pi\hbar)$ is 10.1 MHz at 334 G, which is larger than the result from the complex energy by about 6%. The frequency $\Gamma_T^{(1)}/(2\pi\hbar)$ increases from 2.76 MHz at 134 G to a maximum of 7.23 MHz at 332 G and then decreases to 2.59 MHz at 494 G. These values are larger than the results from the complex energy by only about 1%.

IV. ^6Li ATOMS: HIGH-FIELD UNIVERSAL REGION

In this section, we apply our formalism to the lowest three hyperfine spin states of ^6Li atoms in the region of high magnetic field from 600 to 1200 G. In Fig. 4, the three scattering lengths a_{12} , a_{23} , and a_{13} are shown as functions of the magnetic field [42]. This

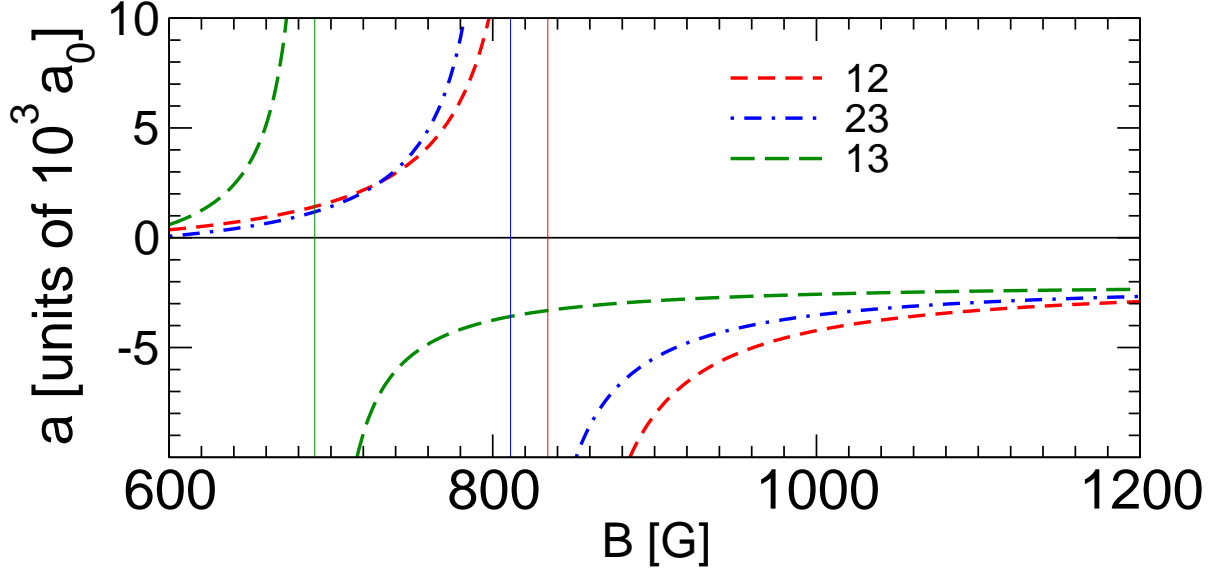


FIG. 4: (Color online) The scattering lengths in units of $10^3 a_0$ for the three lowest hyperfine states of ^6Li as functions of the magnetic field B from 600 G to 1200 G [42]. The three vertical lines mark the positions of the Feshbach resonances.

region includes the Feshbach resonances in a_{12} , a_{23} , and a_{13} near 834 G, 811 G, and 690 G, respectively. Beyond these Feshbach resonances, all three scattering lengths approach the triplet scattering length $-2140 a_0$. For $B > 637$ G, the absolute values of all three scattering lengths are larger than $2140 a_0 \approx 34 \ell_{\text{vdW}}$. An estimate of the lower boundary of this universal region is 608 G, where the smallest scattering length is $a_{13} = 125 a_0 \approx 2 \ell_{\text{vdW}}$. The zero-range approximation should be very accurate throughout most of this high-field region. The physics in this universal region is rich, with the Feshbach resonances marking the boundaries between regions in which 3, 2, 1, or 0 of the three scattering lengths are positive.

A. Measurements of Three-body Recombination

In Ref. [27], Huckans et al. presented measurements of the 3-body recombination rate at 6 values of the magnetic field in the range 600 G to 1000 G. The low-temperature limit of the recombination rate could not be measured, because the temperature was not low enough and because of heating associated with the Feshbach resonance. In Ref. [28], we showed that a naive fit of the last two data points at 894 G and 953 G using our zero-temperature calculations indicated an Efimov resonance near 1200 G. We suggested that it might be worthwhile to search the high-field region for an Efimov resonance.

A narrow 3-atom loss resonance in the high-field region near 895 G was recently discovered by Williams et al. [31] and by Jochim and coworkers [32]. Williams et al. measured the 3-body recombination rate at magnetic fields from 842 G up to 1500 G at temperatures lower than 180 nK and from 834 G up to 955 G at temperatures lower than 30 nK. Their data is shown in Fig. 5. By fitting their measurements using our formalism, they obtained the 3-body parameters $\kappa_* = (6.9 \pm 0.2) \times 10^{-3} a_0^{-1}$ and $\eta_* = 0.016^{+0.006}_{-0.010}$ [31]. Since κ_* is only defined up to multiplication by integer powers of $\lambda_0 \approx 22.7$, an equivalent value is

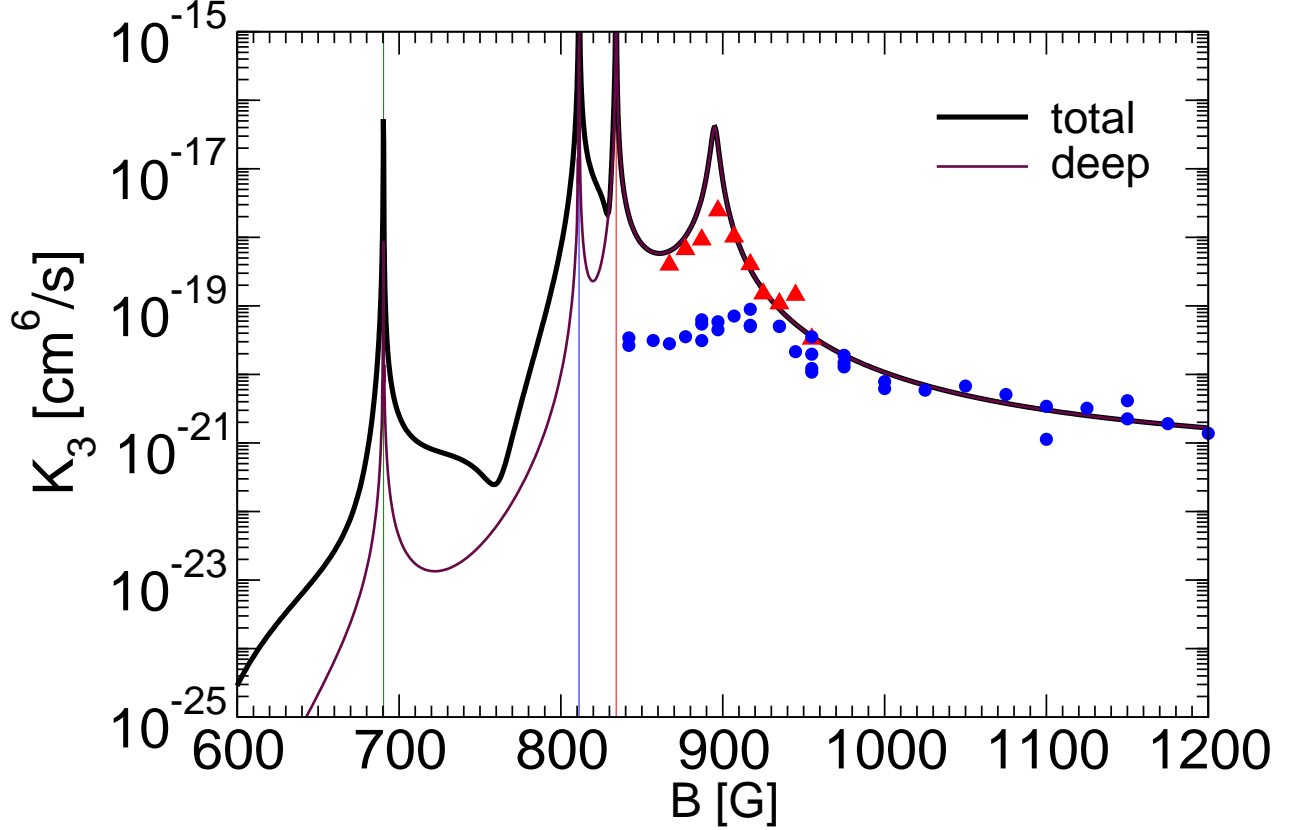


FIG. 5: (Color online) Three-body recombination rate constant K_3 as a function of the magnetic field B from 600 G to 1200 G. The solid dots and triangles are data points from Ref. [27] at temperatures less than 180 nK and less than 30 nK, respectively. The curve between 834 G and 1200 G is a fit to that data. In the region from 600 G and 834 G, the curves are our predictions for the total 3-body recombination rate (thick line) and the contribution from recombination into deep dimers (thin line) for $\kappa_* = 80.7 a_0^{-1}$ and $\eta_* = 0.016$. The three vertical lines mark the positions of the Feshbach resonances.

$\kappa_* = 80.7 \pm 2.3 a_0^{-1}$. Their fit for the central values of κ_* and η_* is shown in Fig. 5 as the thick solid line between 834 G and 1200 G. The fitted value for the position of the 3-atom loss resonance is 895_{-5}^{+4} G. The peak value of the 3-body recombination rate at zero temperature is predicted to be $(4.1_{-1.5}^{+8.5}) \times 10^{-17} \text{ cm}^6/\text{s}$.

It is interesting to compare the values of the 3-body parameters κ_* and η_* in the high-field region with those in the low-field region. The values in the low-field region obtained by fitting the measurements of the narrow 3-body recombination loss feature by Ottenstein et al. [26] were $\kappa_* \approx 76.8 a_0^{-1}$ and $\eta_* \approx 0.11$. It is difficult to quantify the errors in these parameters, because the narrow loss feature is at the edge of the universal region where range corrections may be significant. The values of κ_* in the high-field region and the low-field region are consistent within errors. This could be just a coincidence, but it suggests that the phase in the 3-body wavefunction at short distances that controls Efimov physics is insensitive to the Feshbach resonances that change the scattering lengths. The value of η_* in the high-field region is about an order-of-magnitude smaller than in the low-field region. This demonstrates that the 3-body parameters need not be equal in the two universal

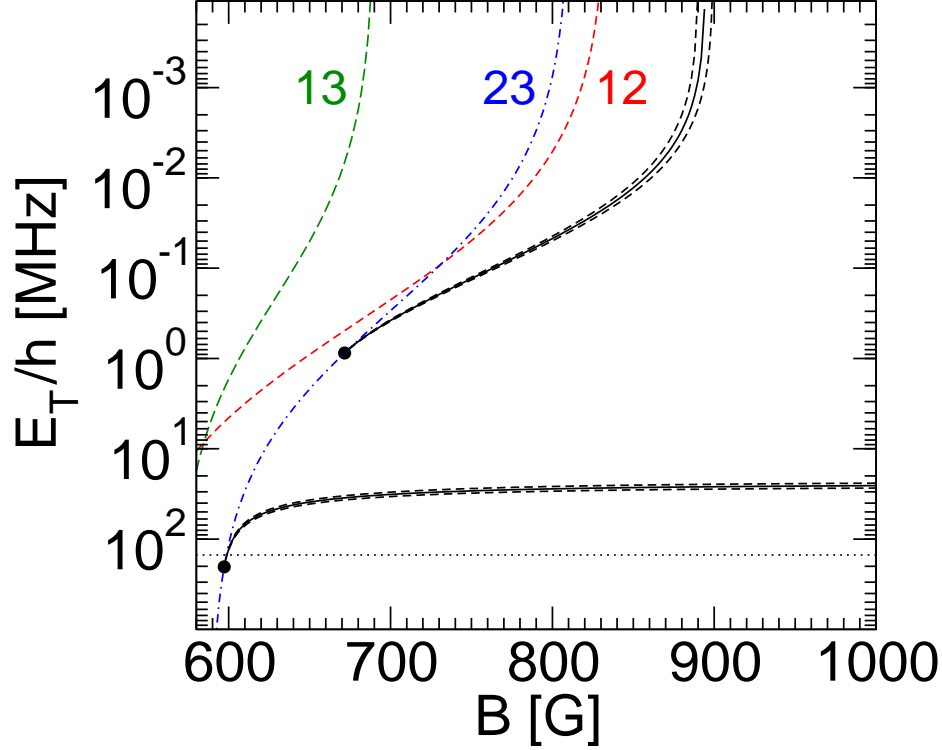


FIG. 6: (Color online) Energies of the Efimov trimers as functions of the magnetic field B in the high-field region. The solid curves are the predicted binding frequencies $E_T^{(n)}/(2\pi\hbar)$ for $\kappa_* = 80.7 \text{ } a_0^{-1}$ and $\eta_* = 0.016$. The dashed curves are the upper and lower error bars obtained by varying κ_* . The curves labelled 12, 23, and 13 are the atom-dimer thresholds. The dots indicate the points where the trimers disappear through the $1+(23)$ atom-dimer threshold. The horizontal dotted line is the van der Waals frequency 154 MHz.

regions. Wenz et al. proposed a mechanism for variations in η_* , namely significant changes in the binding energies of deep dimers with the magnetic field [43]. This mechanism might also explain the order-of-magnitude difference in η_* between the two regions.

Using the values of κ_* and η_* determined by O'Hara et al. [31], we can calculate the universal predictions for other aspects of Efimov physics for ^6Li atoms in the high-field universal region. The error bars on the values of κ_* and η_* can be used to give error bars on the predictions. In the next subsections, we give universal predictions for the binding energies and the widths of the Efimov trimers and for the 3-body recombination rate.

B. Efimov Trimers

We calculate the binding energies and the widths of the Efimov trimers by solving for the complex energy eigenvalues of the homogeneous STM equations in Eq. (22). We choose to label the Efimov trimer responsible for the narrow loss feature near 895 G by the integer $n = 1$. In Fig. 6, the predicted binding energies $E_T^{(0)}$ and $E_T^{(1)}$ of the two shallowest Efimov trimers are shown as functions of the magnetic field. The Efimov trimer responsible for the narrow loss feature has a binding energy $E_T^{(1)}$ that vanishes at 895_{-5}^{+4} G. As the magnetic field

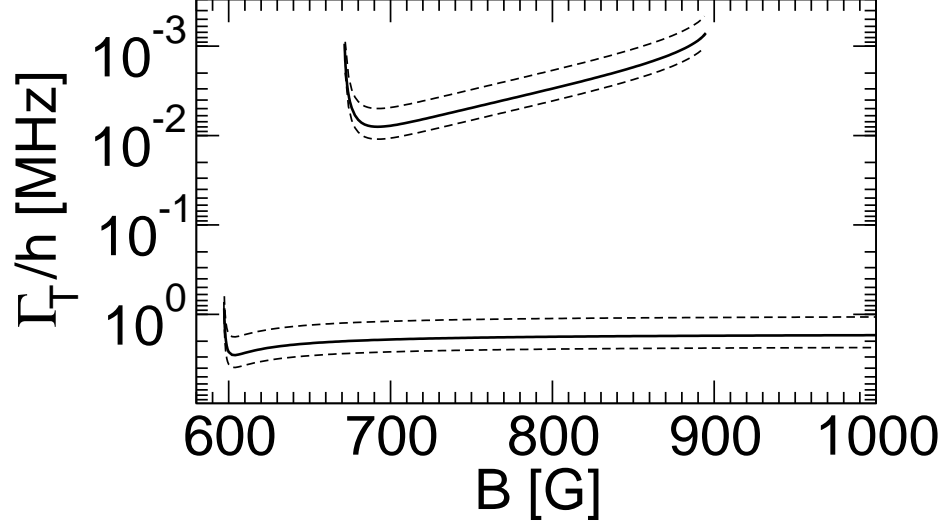


FIG. 7: Widths of the Efimov trimers as functions of the magnetic field B in the high-field region. The solid curves are the frequencies $\Gamma_T^{(n)}/(2\pi\hbar)$ associated with the widths for $\kappa_* = 80.7 a_0^{-1}$ and $\eta_* = 0.016$. The dashed curves are the upper and lower error bars obtained by varying η_* .

decreases, $E_T^{(1)}$ increases monotonically until the critical value $B_* = 672 \pm 2$ G where the Efimov trimer disappears through the $1+(23)$ atom-dimer threshold. When it disappears, its binding energy $E_T^{(1)}$ relative to the 3-atom threshold is 871_{-68}^{+43} kHz, which is also the binding energy $\hbar^2/(ma_{23}^2)$ of the (23) dimer. The next deeper Efimov trimer has a binding frequency $E_T^{(0)}/(2\pi\hbar)$ that increases monotonically from $26.4_{-1.6}^{+1.7}$ MHz at 895 G to $34.9_{-1.9}^{+1.9}$ MHz at B_* . Our solutions to the STM equations predict that it crosses the $1+(23)$ atom-dimer threshold at 597 G, where its binding frequency relative to the 3-atom threshold is 203 MHz. This frequency is larger than the van der Waals frequency 154 MHz. Moreover the smallest scattering length at this point is only $54 a_0$, which is smaller than the van der Waals length $65 a_0$. The zero-range predictions are not expected to be accurate for such large energies and for such small scattering lengths. All the deeper Efimov trimers have binding energies that are much larger than the van der Waals energy and are therefore artifacts of the zero-range approximation. Our value of κ_* can be interpreted as the binding wavenumber $(mE_T^{(-2)}/\hbar^2)^{1/2}$ of the fictitious Efimov trimer labelled by $n = -2$. It corresponds to the choice $n_* = -2$ in Eq. (1).

As discussed in Sec. III C, the leading range corrections to the binding energy for the deep trimers are estimated to be of order $\ell_{vdW}(mE_T^{(n)}/\hbar^2)^{1/2}$. For the trimer labeled $n = 1$, these corrections are 8% where it crosses the $1+(23)$ atom-dimer threshold and become significantly smaller at larger values of the magnetic field. For the trimer labelled $n = 0$ these corrections are about 40% at B_* and larger values of the magnetic field.

In Fig. 7, the predicted widths $\Gamma_T^{(n)}$ of the Efimov trimers are shown as functions of the magnetic field. The frequency $\Gamma_T^{(1)}/(2\pi\hbar)$ associated with the width of the shallower trimer increases from 0.706 kHz at 895 G to a maximum of 7.98 kHz at 692 G and then decreases to 0.940 kHz at B_* . The frequency $\Gamma_T^{(0)}/(2\pi\hbar)$ associated with the width of the deeper trimer increases from 1.74 MHz at 895 G to 2.00 MHz at B_* .

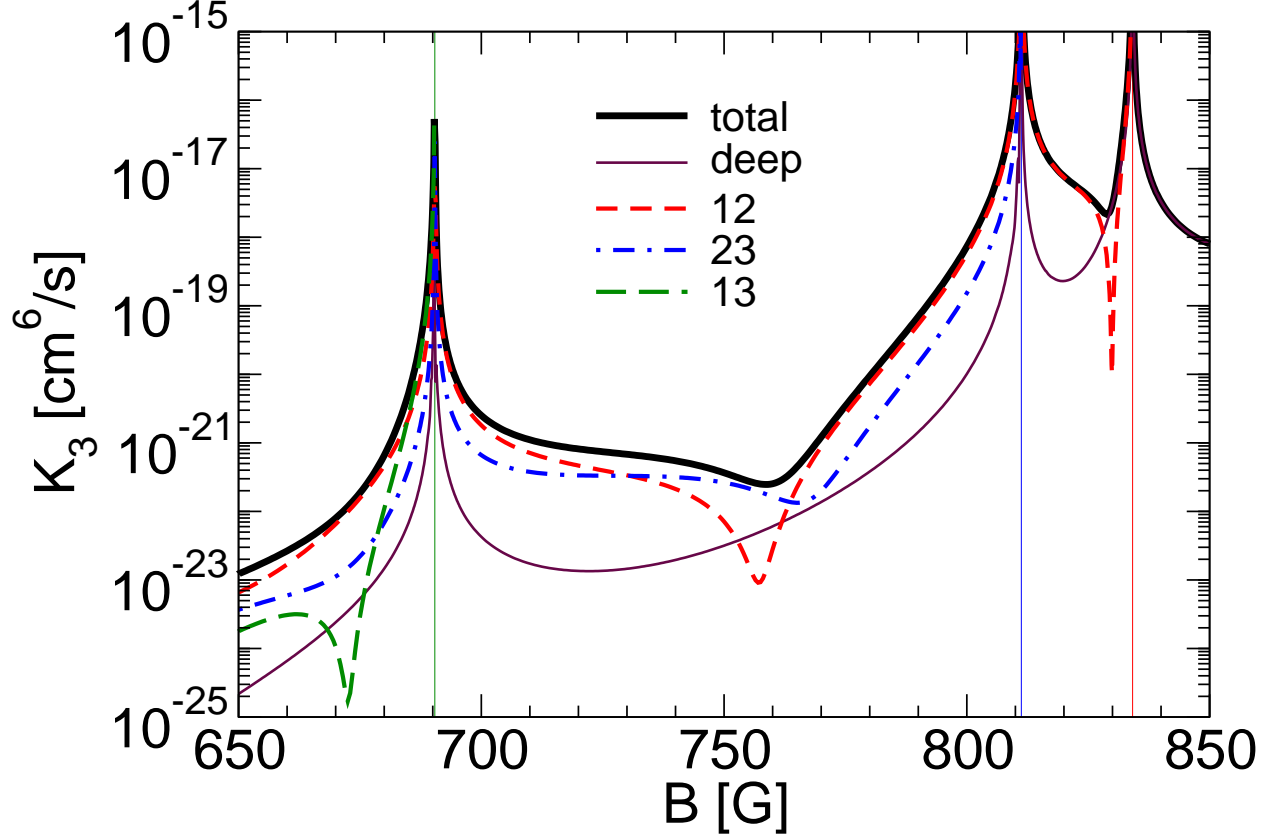


FIG. 8: (Color online) Three-body recombination rate constant K_3 as a function of the magnetic field B from 650 G to 850 G. The curves are our predictions for the total 3-body recombination rate (thick solid line), the contribution from recombination into deep dimers (thin solid line), and the contributions from recombination into the (12) dimer (short-dashed line), the (23) dimer (dash-dotted line), and the (13) dimer (long-dashed line) for $\kappa_* = 80.7 a_0^{-1}$ and $\eta_* = 0.016$.

C. Predictions for Three-body Recombination

Our predictions for the 3-body recombination rate in the region 600 G to 834 G, where one or more of the scattering lengths are positive, are shown in Fig. 5. The upper curve is the total recombination rate K_3 , while the lower one is the contribution K_3^{deep} from deep dimers. Besides the Efimov resonance at 895 G, the only other peaks are at the Feshbach resonances at 690 G, 811 G, and 834 G. They arise simply from the scaling of K_3 as a^4 up to logarithms, where a is some appropriate mean of the scattering lengths a_{12} , a_{23} , and a_{13} . The total recombination rate K_3 is predicted to have three local minima. There is a broad local minimum at 759 ± 1 G, where the minimum recombination rate is $(2.5_{-0.5}^{+0.5}) \times 10^{-22}$ cm⁶/s. There is a narrow local minimum at 829 ± 1 G, where the minimum recombination rate is $(2.2_{-1.3}^{+0.9}) \times 10^{-18}$ cm⁶/s. Finally there is a local minimum at 861 ± 2 G between the last Feshbach resonance and the 3-atom Efimov resonance, where the minimum recombination rate is $(5.8_{-4.0}^{+3.8}) \times 10^{-19}$ cm⁶/s.

In Fig. 8, we show the predictions for the 3-body recombination rate in the region from 650 G to 850 G in more detail. In addition to K_3 and K_3^{deep} , we show the contributions from recombination into the (12), (23), and (13) dimers. This figure reveals that the local

minima at 759 G and 829 G are associated with interference in the recombination into shallow dimers. The narrow minimum at 829 G arises from the combination of a rapidly increasing rate into deep dimers and a rapidly decreasing rate into (12) dimers, which has its minimum at 830 G. The broad minimum at 759 G arises from minima in the rates into (12) and (23) dimers at 757 G and 765 G, respectively. There are also minima in the rates into the (13) dimer at 672 G and the (23) dimer at 600 G, but their effects are not visible in the total recombination rate. We have verified that these minima in the recombination rates into individual shallow dimers arise from interference effects by showing that they become zeroes as η_* is decreased to 0. Thus these minima are the result of destructive interference between two recombination pathways. In the case of three equal positive scattering lengths, a similar interference effect is evident in the analytic expression for the 3-body recombination rate into shallow dimers in Eq. (20).

D. Atom-Dimer Resonance

An atom-dimer loss resonance can appear at a value of the scattering length for which an Efimov trimer crosses the atom-dimer threshold. From the Efimov trimer spectrum in Fig. 6, one can see that atom-dimer resonances are predicted at the two values of the magnetic field where the Efimov trimers cross the 1+(23) atom-dimer threshold. The atom-dimer resonance associated with the shallower of the two Efimov trimers is predicted to occur at $B_* = 672 \pm 2$ G. The universal predictions for the dimer relaxation rate near this resonance can be calculated by solving appropriate sets of coupled STM equations. The atom-dimer resonance associated with the deeper of the two Efimov trimers is predicted to occur at $B'_* = 597$ G. This resonance occurs slightly outside the universal region, so universal predictions for the position of the resonance and for the dimer relaxation rate are not expected to be accurate.

If we restrict our attention to magnetic fields very near the atom-dimer resonance at B_* , we can get an approximation to the universal predictions for the dimer relaxation rate $\beta_{1(23)}$ without actually solving the STM equations. We take advantage of the fact that the atom-dimer scattering length $a_{1(23)}$ diverges at B_* . The 3-atom problem in this region therefore reduces to a universal 2-body problem for the atom and the (12) dimer. The universal properties are determined by the large scattering length $a_{1(23)}$. For example, in the region $B > B_*$ but very close to B_* , the binding energy of the Efimov trimer is well approximated by the sum of the binding energy of the (23) dimer and a universal term determined by the atom-dimer scattering length:

$$E_T^{(1)} \approx - \left(\frac{\hbar^2}{ma_{23}^2} + \frac{3\hbar^2}{4ma_{1(23)}^2} \right). \quad (30)$$

This should be a good approximation as long as the second term is much smaller than the first term. In the region near B_* , the atom-dimer scattering length can be approximated by an expression that has the same form as the analytic result for identical bosons but with different numerical coefficients:

$$a_{1(23)} \approx (C_1 \cot[s_0 \ln(a_{23}/a_*) + i\eta_*] + C_2) a_{23}, \quad (31)$$

where $a_* = a_{23}(B_*)$. The coefficients C_1 and C_2 can in principle depend on ratios of the scattering lengths, but a_{13} is an order of magnitude larger so it essentially decouples and a_{13}

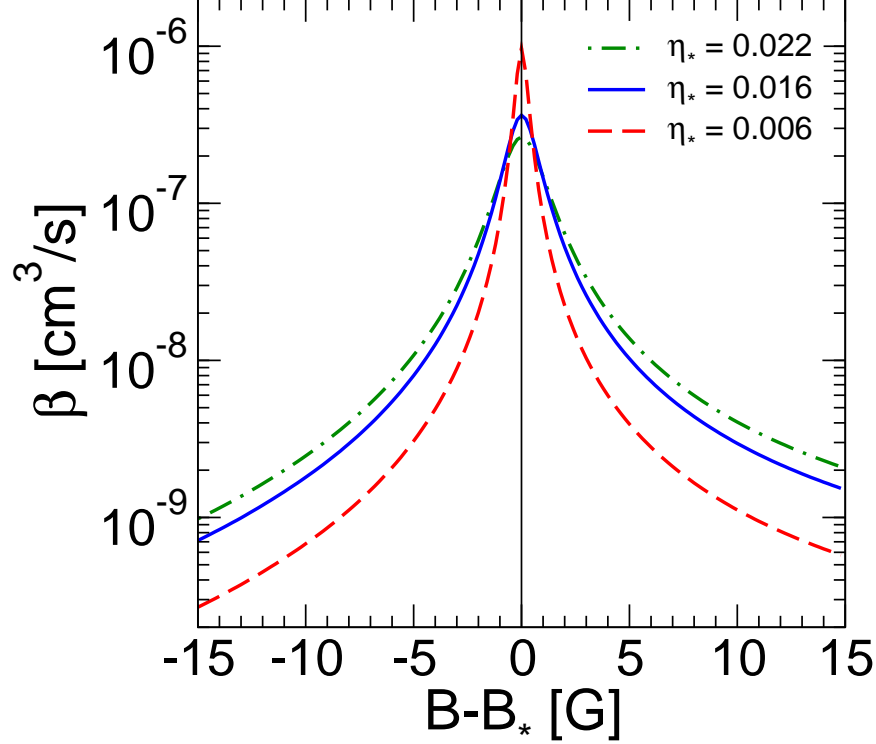


FIG. 9: (Color online) Dimer relaxation rate constant $\beta_{1(23)}$ for (23) dimers and atoms of type 1 as a function of the magnetic field B . The magnetic field is measured relative to the position B_* of the atom-dimer resonance. The curves are predictions using the approximation in Eq. (32) for three values of η_* : 0.006, 0.016, and 0.022.

and a_{23} are both increasing with B so their ratio does not change rapidly near B_* . Thus we can treat C_1 and C_2 as numerical constants. These constants can be determined by using Eq. (30) to extract $a_{1(23)}$ from the results for the real part of the trimer binding energy shown in Fig. 6 and then fitting those results to the expression for the atom-dimer scattering length in Eq. (31). The resulting constants are $C_1 = 0.67$ and $C_2 = 0.65$.

With the constant C_1 in hand, we can obtain an approximation for the dimer relaxation rate constant $\beta_{1(23)}$ for B near B_* simply by inserting the approximation for $a_{1(23)}$ in Eq. (31) into the optical theorem relation in Eq. (27). The resulting expression is

$$\beta_{1(23)} \approx \frac{9.44 C_1 \sinh(2\eta_*)}{\sin^2[s_0 \ln(a_{23}/a_*)] + \sinh^2 \eta_*} \frac{\hbar a_{23}}{m}. \quad (32)$$

If $B_* = 672$ G, the value of a_* is $835 a_0$. The only dependence on the magnetic field is through the B -dependence of a_{23} . This approximation for $\beta_{1(23)}$ is shown as a function of $B - B_*$ in Fig. 9. The maximum value of $\beta_{1(23)}$ at the peak of the resonance is 4×10^{-7} cm³/s for $\eta_* = 0.016$.

Since the atom-dimer resonance associated with the deeper of the two Efimov trimers occurs slightly outside the universal region, universal predictions for the dimer relaxation rate are not expected to be accurate. They might however be useful for making order-of-magnitude estimates. If we apply the analysis described above to the binding energy of the deeper Efimov trimer, we get the constants $C_1 = 0.7$ and $C_2 = 0.3$. The value of a_* is

approximately $54 a_0$. If we use Eq. (32) to estimate the dimer relaxation rate, we obtain a maximum value of $\beta_{1(23)}$ at the peak of the resonance of $2.4 \times 10^{-8} \text{ cm}^3/\text{s}$ for $\eta_* = 0.016$.

E. Many-body physics

One of the most important motivations for understanding few-body physics is that there are aspects of many-body physics that are controlled by few-body observables. Our universal results for the few-body physics of ^6Li atoms with 3 spin states provides useful information about many-body systems of ^6Li atoms with sufficiently low temperature and sufficiently low number densities. If the atoms are in thermal equilibrium at temperature T , an important scale is the thermal length $\lambda_T = (2\pi m k_B T / \hbar^2)^{-1/2}$. If the atoms of type i have number density n_i , another important scale is the Fermi wavenumber $k_{Fi} = (3\pi^2 n_i)^{1/3}$. In our calculation of the 3-body recombination rate, we set the wavenumbers of the incoming atoms to 0. In order for our result to apply quantitatively to all atoms in the system, it is necessary that λ_T^{-1} , k_{F1} , k_{F2} , and k_{F3} all be small compared to the wavenumber scale $(1/a_1^2 + 1/a_2^2 + 1/a_3^2)^{1/2}$ set by the interactions. Even if this condition is not well satisfied, our result can be used to obtain order-of-magnitude estimates of the relevant time scales.

There are several relevant time scales that we can extract from our few-body calculations. If the system contains Efimov trimers, an important time scale is the lifetime $\hbar/\Gamma_T^{(n)}$ of the Efimov trimer, where $\Gamma_T^{(n)}$ is its width. The universal predictions for the widths of the Efimov trimers are shown in Fig. 7. If the system can be approximated by a gas of individual low-energy atoms, the time scale for disappearance of a significant fraction of the atoms is set by the 3-body recombination rate constant K_3 . From the rate equation in Eq. (4), we see that the time scale for loss of a significant fraction of the atoms of type i is $(K_3 n_j n_k)^{-1}$, where j and k are the two complimentary spin states. The universal predictions for the 3-body recombination rate are shown in Figs. 5 and 8. Finally if the system contains low-energy dimers and low-energy atoms in the complimentary spin state, the time scale for disappearance of a significant fraction of the atoms or dimers is set by the appropriate dimer relaxation rate constant. From the rate equation in Eq. (26), we see that the time scales for loss of significant fractions of (23) dimers and of atoms of type 1 are $(\beta_{1(23)} n_1)^{-1}$ and $(\beta_{1(23)} n_{(23)})^{-1}$, respectively. The only universal information we have about dimer relaxation rates is the approximation for $\beta_{1(23)}$ in Eq. (32), which should be accurate for magnetic fields within about 10 G of $B_* \approx 672$ G. For magnetic fields further from this critical value but still within the region where a_{23} is positive, one may be able to use the extrapolation of this expression as an estimate for the dimer relaxation rate.

If the system contains a Bose-Einstein condensate of low-energy dimers as well as low-energy atoms in the complimentary spin state, another important few-body observable is the atom-dimer scattering length for that particular atom and dimer. The real part of the atom-dimer scattering length determines the mean-field energy of the atom in the dimer condensate. The mean-field energy of an atom of type 1 in the (23) dimer condensate with sufficiently low number density $n_{(23)}$ is $(3\pi\hbar^2/m) \text{Re}(a_{1(23)})n_{(23)}$. The approximation for $a_{1(23)}$ in Eq. (31) should be accurate for magnetic fields within about 10 G of $B_* \approx 672$ G.

We will illustrate the relevance of our universal result to many-body physics by applying them to two specific values of the scattering length that are interesting from a symmetry perspective. If the pair scattering lengths a_{ij} and a_{ik} are equal, atoms of types j and k are related by an $SU(2)$ symmetry. If all three scattering lengths are equal, the three spin states

are related by an $SU(3)$ symmetry. There is an $SU(2)$ symmetry point at 731 G, where the scattering lengths are $a_{12} = a_{23} \approx +2500 a_0$ and $a_{13} \approx -7100 a_0$. An $SU(3)$ symmetry point can be approached by going to very high magnetic fields, where all three scattering lengths approach the spin-triplet scattering length $-2140 a_0$ [25].

A quantum degenerate Fermi gas of ^6Li atoms with approximately equal populations of the three lowest hyperfine spin states at 1500 G has been realized by Williams et al. [31]. The scattering lengths are $a_{12} \approx -2460 a_0$, $a_{23} \approx -2360 a_0$, and $a_{13} \approx -2240 a_0$, so there is an approximate $SU(3)$ symmetry. One candidate for a metastable ground state is a state that can be approximated by filled Fermi spheres for all three spin states, with Cooper pairing that breaks the $SU(3)$ symmetry down to a $U(1)$ subgroup. The lifetime for such a system is determined by the 3-body recombination rate K_3 , which is predicted to be about $8 \times 10^{-22} \text{ cm}^6/\text{s}$ at 1500 G. Another candidate for a metastable ground state is a filled Fermi sphere of Efimov trimers. The binding energy $E_T^{(0)}$ of the Efimov trimer is predicted to be about $25 \text{ MHz} \times (2\pi\hbar)$ at 1500 G. Its width $\Gamma_T^{(0)}$ is predicted to be about $1.7 \text{ MHz} \times (2\pi\hbar)$, which corresponds to a lifetime $\hbar/\Gamma_T^{(0)}$ of about $9 \times 10^{-8} \text{ s}$.

We now consider a many-body system at 731 G, where there is an $SU(2)$ symmetry relating the atoms of types 1 and 3. For a state that can be approximated by filled Fermi spheres for all three spin states, the lifetime is determined by the 3-body recombination rate K_3 , which is predicted to be about $7 \times 10^{-22} \text{ cm}^6/\text{s}$ at 731 G. A better candidate for a metastable ground state is a state containing a Bose-Einstein condensate of dimers, which breaks the $SU(2)$ symmetry down to a $U(1)$ subgroup, and a filled Fermi sphere of the complimentary atoms. The lifetime of the state is determined by the dimer relaxation rates $\beta_{1(23)}$ and $\beta_{3(12)}$, which are equal by the $SU(2)$ symmetry. We can estimate $\beta_{1(23)}$ by extrapolating the expression for the dimer relaxation rate $\beta_{1(23)}$ in Eq. (32) to 731 G, which gives $3 \times 10^{-10} \text{ cm}^3/\text{s}$. We can also estimate the mean-field energy of an atom of type 1 in a (23) dimer condensate with number density $n_{(23)}$ by extrapolating the expression for the atom-dimer scattering length $a_{1(23)}$ in Eq. (31) to 731 G. The resulting estimate is $2 \times 10^{-9} \text{ Hz cm}^3 \times (2\pi\hbar n_{(23)})$. The positive sign of the real part of $a_{1(23)}$ implies that the atoms of type 1 are repelled by the (23) dimer condensate. A state in which the dimer condensate and the atoms are spatially separated is therefore energetically favored over a homogeneous state. A final candidate for a metastable ground state is a filled Fermi sphere of Efimov trimers. The binding energy $E_T^{(1)}$ of the shallower Efimov trimer is predicted to be about $190 \text{ kHz} \times (2\pi\hbar)$ at 731 G. Its width $\Gamma_T^{(1)}$ is predicted to be about $6 \text{ kHz} \times (2\pi\hbar)$ at 731 G, which corresponds to a lifetime $\hbar/\Gamma_T^{(1)}$ of about $3 \times 10^{-5} \text{ s}$.

V. SUMMARY

Systems consisting of ^6Li atoms with 3 spin states provide a rich playground for the interplay between few-body physics and many-body physics. The experimental study of many-body physics is only possible if the loss rates of atoms from few-body processes are sufficiently low. Measurements of the position and width of a single Efimov loss feature can be used to determine the 3-body parameters κ_* and η_* . Calculations in the zero-range limit can then be used to predict few-body reaction rates in the entire universal region.

In the low-field region for ^6Li atoms, the universal predictions were only qualitatively successful. A fit to the measurements of the 3-body recombination rate by Ottenstein et al. gives the 3-body parameters $\kappa_* \approx 77 a_0^{-1}$ and $\eta_* \approx 0.11$. With these parameters, the

universal results for the 3-body recombination rate as a function of the magnetic field give a good fit to the narrow loss feature near 130 G but do not agree well with measurements in the upper half of the low-field region [28–30]. A reasonable explanation was proposed by Wenz et al. [43]: η_* is particularly sensitive to the binding energies of the shallowest of the deep dimers and there are ^6Li dimers whose binding energies change dramatically across the low-field region. Assuming the scaling behavior $\eta_* \sim E_{\text{deep}}^{-1}$, they obtained a good fit to the recombination rate in the low-field region.

In the high-field region for ^6Li atoms, the scattering lengths are much larger so the universal predictions should be much more accurate. A narrow 3-atom loss feature near 895 G was discovered by Williams et al. [31] and by Jochim and coworkers [32]. By fitting their measurements of the 3-body recombination rate, Williams et al. determined the 3-body parameters associated with Efimov physics to be $\kappa_* = 80.7 \pm 2.3 \text{ } a_0^{-1}$ and $\eta_* = 0.016^{+0.006}_{-0.010}$. We used those parameters to calculate the universal predictions for the binding energies and widths of the Efimov trimers shown in Fig. 6 and 7. The Efimov trimer responsible for the narrow loss feature is predicted to disappear through the $1+(23)$ atom-dimer threshold at 672 ± 2 G, producing a spectacular atom-dimer loss resonance. There is also a deeper Efimov trimer whose binding frequency and width in the universal region are approximately 30 MHz and $2 \text{ MHz} \times (2\pi\hbar)$, respectively. This trimer is also predicted to disappear through the $1+(23)$ atom-dimer threshold, but this happens outside the universal region. We also used the 3-body parameters determined by Williams et al. to calculate the universal predictions for the 3-body recombination rate, which are shown in Figs. 5 and 8. Local minima in K_3 are predicted at 759 ± 1 G, 829 ± 1 G, and 861 ± 1 G. Finally an approximate calculation of the dimer relaxation rate in the region of the atom-dimer resonance is presented in Fig. 9. We look forward to the experimental verification of these predictions.

In order to understand the behavior of atom-dimer mixtures at low temperatures, it would be useful to have universal predictions for other 3-atom observables. They include the atom-dimer scattering lengths, which are in general complex. The real part of an atom-dimer scattering length determines the mean-field shifts of the atom in the dimer condensate. Its imaginary part is proportional to the dimer relaxation rate. For the shallow dimer with the largest binding energy, which is the (23) dimer for $B < 730$ G and the (12) dimer for $730 \text{ G} < B < 834$ G, the only relaxation channels are into deep dimers. For shallow dimers with smaller binding energy, there are also relaxation channels into other shallow dimers. It would be especially useful to have definitive universal predictions for the relaxation rate constant $\beta_{1(23)}$ near the predicted atom-dimer threshold at 672 ± 2 G. It would improve upon the approximation illustrated in Fig. 9 by taking into account the B -dependence of the ratios of scattering lengths.

There have not yet been any direct observations of Efimov trimers in ultracold atoms. They have only been observed indirectly through the resonant enhancement of 3-body recombination and through the resonant enhancement of atom-dimer relaxation provided by virtual Efimov trimers. The direct production of Efimov trimers would be another milestone in the study of Efimov physics in ultracold atoms. Of course, once they are produced, they would decay quickly. In the high-field universal region for ^6Li atoms, the deeper Efimov trimer is predicted to have a very short lifetime of about 10^{-7} s. The shallower Efimov trimer is predicted to have a lifetime of 10^{-4} s to 10^{-5} s. Our universal predictions for the binding energies of these Efimov trimers should be useful in devising experimental strategies for producing them.

Acknowledgments

We thank S. Jochim and K.M. O’Hara for useful communications. This research was supported in part by the DOE under grants DE-FG02-05ER15715 and DE-FC02-07ER41457, by a joint grant from AFOSR and ARO, by the NSF under grant PHY-0653312, by the BMBF under contracts 06BN411 and 06BN9006, and by the Alexander von Humboldt Foundation.

-
- [1] *Ultracold Fermi Gases*, ed. M. Inguscio, W. Ketterle, and C. Salomon (IOS Press, Amsterdam, 2008).
 - [2] P.F. Bedaque and J.P. D’Incao, *Annals Phys.* **324**, 1763 (2009) [arXiv:cond-mat/0602525].
 - [3] T. Paananen, J.-P. Martikainen, and P. Törmä, *Phys. Rev. A* **73**, 053606 (2006) [arXiv:cond-mat/0603498].
 - [4] L. He, M. Jin, and P. Zhuang, *Phys. Rev. A* **74**, 033604 (2006) [arXiv:cond-mat/0604580].
 - [5] H. Zhai, *Phys. Rev. A* **75**, 031603(R) (2007) [arXiv:cond-mat/0607459].
 - [6] J.-P. Martikainen, J. Kinnunen, P. Torma, and C.J. Pethick, arXiv:0908.3733.
 - [7] V. Efimov, *Phys. Lett.* **33B**, 563 (1970).
 - [8] E. Braaten and H.-W. Hammer, *Phys. Rept.* **428**, 259 (2006) [arXiv:cond-mat/0410417].
 - [9] E. Braaten and H.-W. Hammer, *Annals Phys.* **322**, 120 (2007) [arXiv:cond-mat/0612123].
 - [10] L. Platter, *Few-Body Syst.* **46**, 139 (2009), [arXiv:0904.2227].
 - [11] V. Efimov, *Nucl. Phys. A* **210**, 157 (1973).
 - [12] T. Kraemer, M. Mark, P. Waldburger, J.G. Danzl, C. Chin, B. Engeser, A.D. Lange, K. Pilch, A. Jaakkola, H.-C. Nägerl, and R. Grimm, *Nature* **440**, 315 (2006) [arXiv:cond-mat/0611629].
 - [13] E. Nielsen and J.H. Macek, *Phys. Rev. Lett.* **83**, 1566 (1999).
 - [14] B.D. Esry, C.H. Greene, and J.P. Burke, *Phys. Rev. Lett.* **83**, 1751 (1999).
 - [15] P.F. Bedaque, E. Braaten, and H.-W. Hammer, *Phys. Rev. Lett.* **85**, 908 (2000) [arXiv:cond-mat/0002365].
 - [16] E. Braaten and H.-W. Hammer, *Phys. Rev. A* **70**, 042706 (2004) [arXiv:cond-mat/0303249].
 - [17] S. Knoop, F. Ferlaino, M. Mark, M. Berninger, H. Schoebel, H.-C. Nägerl, and R. Grimm, *Nature Physics* **5**, 227 (2009) [arXiv:0807.3306].
 - [18] K. Helfrich and H.-W. Hammer, *Europhys. Lett.* **86**, 53003 (2009) [arXiv:0902.3410].
 - [19] H.-W. Hammer and L. Platter, *Eur. Phys. J. A* **32**, 113 (2007) [arXiv:nucl-th/0610105].
 - [20] J. von Stecher, J. P. D’Incao, and C. H. Greene, *Nature Physics* **5**, 417 (2009) [arXiv:0810.3876].
 - [21] F. Ferlaino, S. Knoop, M. Berninger, W. Harm, J. P. D’Incao, H.-C. Nägerl, R. Grimm, *Phys. Rev. Lett.* **102**, 140401 (2009) [arXiv:0903.1276].
 - [22] M. Zaccanti, B. Deissler, C. D’Errico, M. Fattori, M. Jona-Lasinio, S. Müller, G. Roati, M. Inguscio, and G. Modugno, *Nature Physics* **5**, 586 (2009) [arXiv:0810.3876].
 - [23] G. Barontini, C. Weber, F. Rabatti, J. Catani, G. Thalhammer, M. Inguscio, and F. Minardi, *Phys. Rev. Lett.* **103**, 043201 (2009) [arXiv:0901.4584].
 - [24] N. Gross, Z. Shotan, S. Kokkelmans, L. Khaykovich, *Phys. Rev. Lett.* **103**, 163202 (2009) [arXiv:0906.4731].
 - [25] M. Bartenstein, A. Altmeyer, S. Riedl, R. Geursen, S. Jochim, C. Chin, J. Hecker Denschlag, R. Grimm, A. Simoni, E. Tiesinga, C.J. Williams, and P.S. Julienne, *Phys. Rev. Lett.* **94**, 103201 (2005) [arXiv:cond-mat/0408673].

- [26] T.B. Ottenstein, T. Lompe, M. Kohnen, A.N. Wenz, and S. Jochim, Phys. Rev. Lett. **101**, 203202 (2008) [arXiv:0806.0587].
- [27] J. H. Huckans, J. R. Williams, E. L. Hazlett, R. W. Stites and K. M. O'Hara, Phys. Rev. Lett. **102**, 165302 (2009) [arXiv:0810.3288].
- [28] E. Braaten, H.-W. Hammer, D. Kang and L. Platter, Phys. Rev. Lett. **103**, 073202 (2009) [arXiv:0811.3578].
- [29] P. Naidon and M. Ueda, Phys. Rev. Lett. **103**, 073203 (2009) [arXiv:0811.4086].
- [30] R. Schmidt, S. Floerchinger, and C. Wetterich, Phys. Rev. A **79**, 053633 (2009) [arXiv:0812.1191].
- [31] J.R. Williams, E.L. Hazlett, J.H. Huckans, R.W. Stites, Y. Zhang, and K.M. O'Hara, arXiv:0908.0789.
- [32] S. Jochim, private communication.
- [33] D.S. Petrov, Phys. Rev. A **67**, 010703(R) (2003) [arXiv:cond-mat/0209246].
- [34] J.P. D'Incao and B.D. Esry, Phys. Rev. Lett. **94**, 213201 (2005) [arXiv:cond-mat/0411565].
- [35] G.V. Skorniakov and K.A. Ter-Martirosian, Sov. Phys. JETP **4**, 648 (1957) [J. Exptl. Theoret. Phys. (U.S.S.R.) **31**, 775 (1956)].
- [36] H.-W. Hammer and T. Mehen, Nucl. Phys. A **690**, 535 (2001) [arXiv:nucl-th/0011024].
- [37] E. Braaten, H.-W. Hammer and T. Mehen, Phys. Rev. Lett. **88**, 040401 (2002) [arXiv:cond-mat/0108380].
- [38] A.O. Gogolin, C. Mora, and R. Egger, Phys. Rev. Lett. **100**, 140404 (2008).
- [39] J.H. Macek, S. Ovchinnikov, and G. Gasaneo, Phys. Rev. A **72**, 032709 (2005).
- [40] D. Petrov, talk at the Workshop on Strongly Interacting Quantum Gases, Ohio State University, April 2005.
- [41] D.S. Petrov, C. Salomon, and G.V. Shlyapnikov, Phys. Rev. Lett. **93**, 090404 (2004) [arXiv:cond-mat/0309010].
- [42] P.S. Julienne, private communication (2009).
- [43] A.N. Wenz, T. Lompe, T.B. Ottenstein, F. Serwane, G. Zürn, and S. Jochim, Phys. Rev. A **80**, 040702 (2009) [arXiv:0906.4378].
- [44] E. Braaten and D. Kang, in preparation.